

See discussions, stats, and author profiles for this publication at: <https://www.researchgate.net/publication/51095267>

# Tightening of Active Site Interactions En Route to the Transition State Revealed by Single-Atom Substitution in the Guanosine-Binding Site of the Tetrahymena Group I Ribozyme

ARTICLE *in* JOURNAL OF THE AMERICAN CHEMICAL SOCIETY · MAY 2011

Impact Factor: 12.11 · DOI: 10.1021/ja111316y · Source: PubMed

---

CITATIONS

4

---

READS

19

## 4 AUTHORS, INCLUDING:



**Marcello Forconi**

College of Charleston

19 PUBLICATIONS 251 CITATIONS

SEE PROFILE



**Daniel Herschlag**

Stanford University

287 PUBLICATIONS 16,539 CITATIONS

SEE PROFILE

# Tightening of Active Site Interactions En Route to the Transition State Revealed by Single-Atom Substitution in the Guanosine-Binding Site of the *Tetrahymena* Group I Ribozyme

Marcello Forconi,<sup>†,||</sup> Rishi H. Porecha,<sup>†</sup> Joseph A. Piccirilli,<sup>‡,§</sup> and Daniel Herschlag<sup>\*,†</sup>

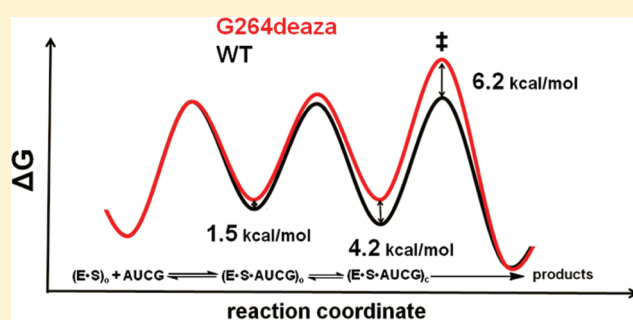
<sup>†</sup>Department of Biochemistry, Stanford University, Stanford, California, United States

<sup>‡</sup>Department of Chemistry and <sup>§</sup>Department of Biochemistry and Molecular Biology, University of Chicago, Chicago, Illinois, United States

 Supporting Information

**ABSTRACT:** Protein enzymes establish intricate networks of interactions to bind and position substrates and catalytic groups within active sites, enabling stabilization of the chemical transition state. Crystal structures of several RNA enzymes also suggest extensive interaction networks, despite RNA's structural limitations, but there is little information on the functional and the energetic properties of these inferred networks. We used double mutant cycles and presteady-state kinetic analyses to probe the putative interaction between the exocyclic amino group of the guanosine nucleophile and the N7 atom of residue G264 of the *Tetrahymena* group I ribozyme. As expected, the results supported the presence of this

interaction, but remarkably, the energetic penalty for introducing a CH group at the 7-position of residue G264 accumulates as the reaction proceeds toward the chemical transition state to a total of 6.2 kcal/mol. Functional tests of neighboring interactions revealed that the presence of the CH group compromises multiple contacts within the interaction network that encompass the reactive elements, apparently forcing the nucleophile to bind and attack from an altered, suboptimal orientation. The energetic consequences of this indirect disruption of neighboring interactions as the reaction proceeds demonstrate that linkage between binding interactions and catalysis hinges critically on the precise structural integrity of a network of interacting groups.



## INTRODUCTION

The discovery of the ability of RNA to act as an enzyme has led to a significant interest in understanding the catalytic strategies used by RNA enzymes, or ribozymes, and in comparing these strategies to those used by the more extensively investigated protein enzymes.<sup>1–3</sup> Studies of several ribozymes have shown that, like protein enzymes, ribozymes bind and position substrates within active sites and use specific interactions to stabilize the reaction's transition state.<sup>1–6</sup> Further, structural studies have provided evidence of extensive networks of interactions within ribozyme active sites, suggesting that ribozymes may be able to use these networks for catalysis.<sup>1</sup> Specifically, these networks might aid the precise positioning of substrates and of the functional groups needed for catalysis.

However, structural inspection alone is insufficient to define the role of these RNA interaction networks in catalysis, especially considering that RNA has limited ability to pack and is known to adopt alternative structures. Further, mutations that remove interactions observed in RNA structures can have small or negligible energetic effects, presumably due to formation of near isoenergetic alternative interactions.<sup>3,7–9</sup> To test the role of networks in RNA catalysis, determination of the energetic consequences of perturbation of both single and multiple

interactions within these networks is needed. We have accomplished this for a network adjoining the active site of the *Tetrahymena* group I ribozyme.

The *Tetrahymena* group I ribozyme has served as a powerful system for uncovering the properties of catalytic RNA. This ribozyme catalyzes a site-specific attack of a guanosine molecule (G) on an oligonucleotide substrate (S), as shown in Figure 1 (for a review of the reaction, see ref 4). In this reaction the oligonucleotide substrate S binds in two steps (Figure 1a). First, S binds to the ribozyme by base-pairing interactions,<sup>10</sup> forming the 'open complex' denoted by the subscript 'o' in Figure 1a. Subsequently, the duplex formed by S and the ribozyme docks in the ribozyme's core to form the 'closed complex' denoted by the subscript 'c' in Figure 1a.<sup>11,12</sup> The closed complex involves tertiary contacts between the substrate–ribozyme duplex (referred to as the P1 helix) and the ribozyme's core.

Guanosine can bind to the free enzyme, the open complex, or the closed complex (Figure 1a). The affinities of G for the free enzyme and the open complex are the same,<sup>13</sup> and this and other observations<sup>14</sup> suggest that the environment around the

Received: December 15, 2010

Published: May 03, 2011

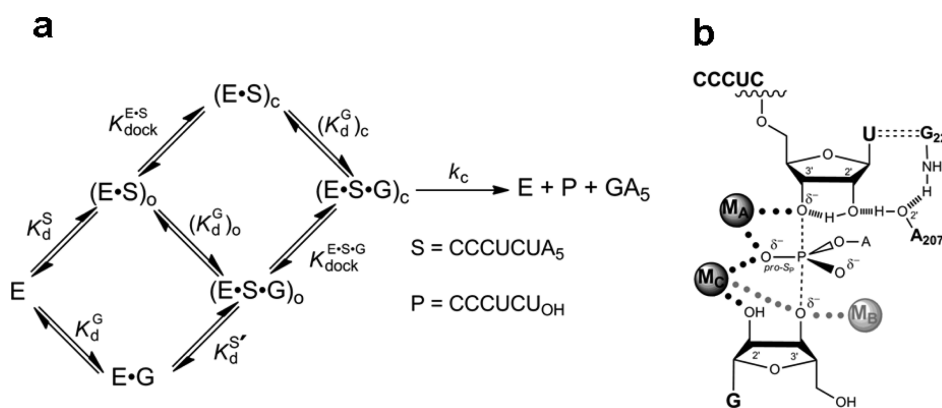


**Figure 1.** A model for the reaction catalyzed by the *Tetrahymena* group I ribozyme. (a) Individual steps of the reaction. The subscript ‘o’ represents the open complex, while the subscript ‘c’ represents the closed complex. (b) Model for the transition state of the reaction. Dashed lines represent hydrogen bonds, dotted lines represent metal ion interaction, and dashed lines represent the bonds broken and formed in the reaction.  $M_A$ ,  $M_B$ , and  $M_C$  represent the three distinct metal ions implicated from functional data.  $M_B$  (higher shading) is not observed in the crystal structures of group I ribozymes, and it has been proposed, based on spatial proximity, that  $M_C$  forms an additional interaction with the 3'-oxygen of the nucleophilic G in the transition state (gray dotted line).

G nucleophile does not change in these two forms of the ribozyme. In contrast, G binds the closed complex  $\sim 5$ -fold more tightly than the open complex, indicating energetic coupling between G binding and docking of the P1 helix.<sup>13</sup> After G is bound and S is docked, the chemical reaction takes place. The reaction involves deprotonation of the 3'-hydroxyl group of G, which then attacks the phosphoryl group between the U and A residues of S. This chemical transformation is assisted by metal ions and other interactions (Figure 1b).<sup>4</sup>

In a seminal paper probing structure–activity relationships in an RNA enzyme, Bass and Cech defined specific atoms or groups on the G nucleophile important for the group I self-splicing reaction.<sup>15</sup> A subsequent specificity switch experiment by Michel and co-workers identified the location of a specific G-binding site, provided evidence for a hydrogen bond between N1 of G and O6 of G264, and suggested the presence of another hydrogen bond between the exocyclic amino group of G and N7 of G264<sup>16</sup> (Figure 2a). Although other models have been proposed,<sup>17,18</sup> these two specific interactions are strongly supported by the proximity of these two groups in all of the structural models derived from group I ribozymes crystallographic data (Figure 2b–d, red and black dashed lines).<sup>19–24</sup>

Here, we have used functional tests, carried out with chemically modified ribozymes and substrates, to investigate the putative interaction between the exocyclic amino group of G and N7 of G264 and the properties of the surrounding environment. Remarkably, perturbation of this interaction has a large energetic effect that accumulates along the reaction trajectory to a value far greater than expected from disruption of a single hydrogen bond. Our results provide powerful functional evidence for the existence of a tight, energetically linked network of interactions surrounding the active site that contributes to the ribozyme's catalytic efficiency and specificity.

## EXPERIMENTAL SECTION

**Materials.** AUCG and AUCI were purchased from Dharmacon Inc. (Lafayette, CO) or synthesized by the PAN Facility (Stanford, CA). AUCG<sub>2'-NH<sub>2</sub></sub> was synthesized at the University of Chicago, using the phosphoramidite of G<sub>2'-NH<sub>2</sub></sub> as previously described.<sup>25</sup> 7-Deazaguanosine phosphoramidite was purchased from ChemGenes (Wilmington, MA).

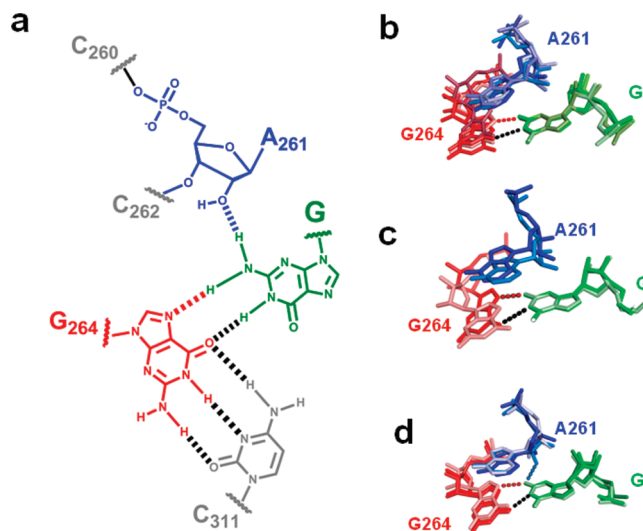


**Figure 2.** The environment around the exocyclic amino group of G in the group I ribozyme. The G nucleophile is in green, residue G264 in red, and residue A261 in blue. Dashed lines represent putative hydrogen bonds. The hydrogen bonds in black and blue are supported by functional data; the putative hydrogen bond represented in red is the interaction studied herein. (a) Two-dimensional chemical representation of the G-binding site. (b) Superposition of the models derived from the *Tetrahymena* group I ribozyme crystals (PDB ID 1X8W), which contain four molecules. (c) Superposition of the models derived from the Twort group I ribozyme crystals (PDB entries 1Y0Q and 2RKJ). (d) Superposition of the models derived from the *Azoarcus* group I ribozyme crystals (PDB entries 1ZZN, 3BO2, and 3BO3). Models were superimposed using the G nucleophile. Residues are numbered using the corresponding numbers from the *Tetrahymena* ribozyme.

Oligonucleotides corresponding to nucleotides 260–274 of the ribozyme, containing a 5'-phosphoryl group, a G or 7-deazaguanosine residue at position 264, and a 2'-OH or 2'-H group at position 261 were synthesized by the PAN Facility (Stanford, CA). Oligonucleotides were purified by reverse-phase HPLC as previously described.<sup>26</sup> Wild type (WT) and variant ribozymes were constructed semisynthetically using a single-step three-piece ligation,<sup>27</sup> with a modified protocol previously described.<sup>26</sup>

**General Kinetic Methods.** All cleavage reactions were single turnover, with ribozyme in excess of radiolabeled oligonucleotide substrate (\*S), which was always present in trace quantities (<100 pM). 5'-<sup>32</sup>P-end-labeling of the oligonucleotide substrates for kinetic experiments was performed by standard methods. The oligonucleotide substrates used in this work are CCCUCdUAAAAA (referred to as -1d,rSA<sub>5</sub>) and d(CCCUC)Ud(AAAAA) (referred to as -1r,dSA<sub>5</sub>). These substrates contain mixed ribose and deoxyribose residues, with deoxyribose residues indicated by a 'd', and allow the reactions to be monitored from different ground-state E·S complexes (see below). Reactions were carried out at 30 °C in 45 mM NaHEPES/5 mM NaMOPS, pH 8.1, and 50 mM MgCl<sub>2</sub>, as previously described.<sup>26</sup>

Kinetic parameters for the WT and A261H ribozymes are from previous work.<sup>26</sup> To obtain the kinetic parameters for the G264deaza and the G264deaza/A261H ribozymes, the rate constant for reaction of \*S was determined as a function of AUCG or AUCI concentration for the different ribozymes. For the G264deaza ribozyme, reactions with up to 4 mM AUCG or with up to 1 mM AUCI were followed. For the G264deaza/A261H ribozyme, up to 300 μM AUCG was used. The ribozyme concentration was 50 nM, and native gels analysis<sup>28,29</sup> confirmed that >95% of \*S was bound to the ribozymes.

For the G264deaza ribozyme, the observed rate constant ( $k_{\text{obs}}$ ) for cleavage of \*S was plotted as a function of AUCG (or AUCI) concentration and fit to eq 1 to obtain  $k_c$ ,  $K_d^{\text{AUCX}}$  and  $(k_{\text{cat}}/K_M)^{\text{AUCX}}$ , where AUCX represents AUCG or AUCI:

$$k_{\text{obs}} = \frac{k_c \times [\text{AUCX}]}{[\text{AUCX}] + K_d^{\text{AUCX}}} \quad (1)$$

For the G264deaza/A261H ribozyme, reactions were performed under subsaturating concentrations of AUCG (0–200 μM), and values of  $(k_{\text{cat}}/K_M)^{\text{AUCG}}$  were by fit to eq 2:

$$k_{\text{obs}} = (k_{\text{cat}}/K_M)^{\text{AUCG}} \times [\text{AUCG}] \quad (2)$$

To determine the kinetic parameters for the closed complex we used the -1d,rSA<sub>5</sub> substrate (CCCUCdUAAAAA). The deoxyribose residue at position -1 ensures that the chemical step is rate limiting and that the observed  $K_{1/2}^{\text{AUCG}}$  (or  $K_{1/2}^{\text{AUCI}}$ ) equals  $(K_d^{\text{AUCG}})_c$  [or  $(K_d^{\text{AUCI}})_c$ ].<sup>13</sup> To determine the kinetic parameters for the open complex, we used the oligonucleotide substrate -1r,dSA<sub>5</sub> [d(CCCUC)Ud(AAAAA)], which favors the open complex because of the absence of specific 2'-OH groups involved in the tertiary interactions that stabilize the closed complex; reaction of this substrate has the chemical step rate limiting, so that the observed rate constant reflects all reaction steps from the open complex ground state to the chemical transition state.<sup>30</sup>

## RESULTS

To test the importance of the putative hydrogen bond between the exocyclic amino group of G and the N7 atom of residue G264 (Figure 2, red dashed line) in the reaction catalyzed by the *Tetrahymena* group I ribozyme, we used double mutant cycles.<sup>31</sup> Specifically, we determined the energetic penalty from removing the exocyclic amino group of the G nucleophile in the context of the WT ribozyme and a ribozyme modified at residue G264 so that it lacks the ability to accept a hydrogen bond at the 7 position. A similar energetic penalty for the WT and modified ribozymes would suggest no functional communication between the G nucleophile and N7 of residue G264 and thus no contact; in contrast, a reduced effect from removing the exocyclic amino group of G in the context of the modified ribozyme would suggest functional communication and, given the proximity observed structurally, a direct contact.

To ablate interactions with the exocyclic amino group of G we used inosine (I) as the nucleophile and to replace the N7 at position G264 of the *Tetrahymena* group I ribozyme with a group no longer capable of acting as hydrogen-bond acceptor, we constructed a semisynthetic ribozyme variant containing a CH group at the 7-position of residue 264 (see Experimental Section), referred to herein as the G264deaza ribozyme. To serve as a control for potential effects of the semisynthetic procedure, we constructed a semisynthetic variant of the WT ribozyme. This construct gave kinetic behavior identical to the transcribed WT ribozyme (data not shown), as found in other ribozyme constructs ligated by similar procedures.<sup>26,32–36</sup> Because of the low solubility of G relative to its dissociation constant,<sup>13,37</sup> we used a G analog, AUCG, instead of G; similarly we used AUCI instead of inosine. These analogs exhibit tighter binding without altering the reaction mechanism.<sup>38,39</sup>

**Testing the Putative Interaction between the Exocyclic Amino Group of the Nucleophile and the N7 Atom of Residue G264.** To determine the energetic consequence of removing the exocyclic amino group of AUCG in the context of the WT and the G264deaza ribozymes, we measured the second-order rate constant,  $(k_{\text{cat}}/K_M)^{\text{AUCX}}$ , for reactions of the two ribozymes, where the superscript AUCX denotes AUCG or AUCI. The constant  $(k_{\text{cat}}/K_M)$  is determined by all reaction steps from free enzyme and substrate up to and including the first irreversible step. Because the chemical step is the first irreversible step under all of the conditions used in this work,<sup>30</sup> the value of  $(k_{\text{cat}}/K_M)$  is affected by this step and all steps that precede it, which are S binding, AUCG (or AUCI) binding, and S docking (Figure 1a). We monitored the reactions under conditions in which the oligonucleotide (S) is already bound to the ribozyme in the so-called open complex [(E·S)<sub>o</sub>, Figure 1a], because the open complex gives a defined state that involves only base pairing of S with the ribozyme that is not expected to be affected by modifications in the G binding site.<sup>10,40,41</sup> To favor the open complex, we used the oligonucleotide substrate -1r,dSA<sub>5</sub> (see General Kinetic Methods Section), in which specific 2'-OH groups that stabilize the docked state are replaced by 2'-H groups.

The interaction tested is represented by the red dashed line in Figure 3 and is enclosed by a black rectangle. The other interactions made by the G nucleophile and shown in Figure 3 have been established by previous functional data<sup>15,16,26,36</sup> and are consistent with X-ray crystal structures.<sup>19–24</sup> Figure 3 also summarizes the overall effects of the atomic perturbations on catalysis, showing the  $(k_{\text{cat}}/K_M)^{\text{AUCX}}$  values for each of the four combinations of ribozyme and nucleophile, with these values converted into free energy differences as described in Figure 3 legend. Previous results have shown that AUCI reacts ~230-fold slower than AUCG in the WT ribozyme [Figure 3,  $(k_{\text{cat}}/K_M)^{\text{AUCG}}_{\text{open}} = 93\,000\text{ M}^{-1}\text{min}^{-1}$  and  $(k_{\text{cat}}/K_M)^{\text{AUCI}}_{\text{open}} = 410\text{ M}^{-1}\text{min}^{-1}$ ], corresponding to an energetic penalty of 3.3 kcal/mol [ $\Delta\Delta G(k_{\text{cat}}/K_M)^{\text{NH}_2 \rightarrow \text{H}}$ ].<sup>26,36</sup> Based on the interactions observed in the crystal structures,<sup>20–22,24</sup> this energy would correspond to the loss of two hydrogen bonds that are formed between the exocyclic amino group of G and the ribozyme, modulated by any contributions from favorable or unfavorable changes in solvation and from steric effects upon complex formation. In contrast, we found that AUCI reacts 1200-fold faster than AUCG in the G264deaza ribozyme [Figure 3,  $(k_{\text{cat}}/K_M)^{\text{AUCG}}_{\text{open}} = 3\text{ M}^{-1}\text{min}^{-1}$  and  $(k_{\text{cat}}/K_M)^{\text{AUCI}}_{\text{open}} = 3600\text{ M}^{-1}\text{min}^{-1}$ ], corresponding to an energetic gain of 4.2 kcal/mol [ $\Delta\Delta G(k_{\text{cat}}/K_M)^{\text{NH}_2 \rightarrow \text{H}}_{\text{CH}}$ ]. The observed coupling in the double mutant cycle suggests that the interaction is indeed



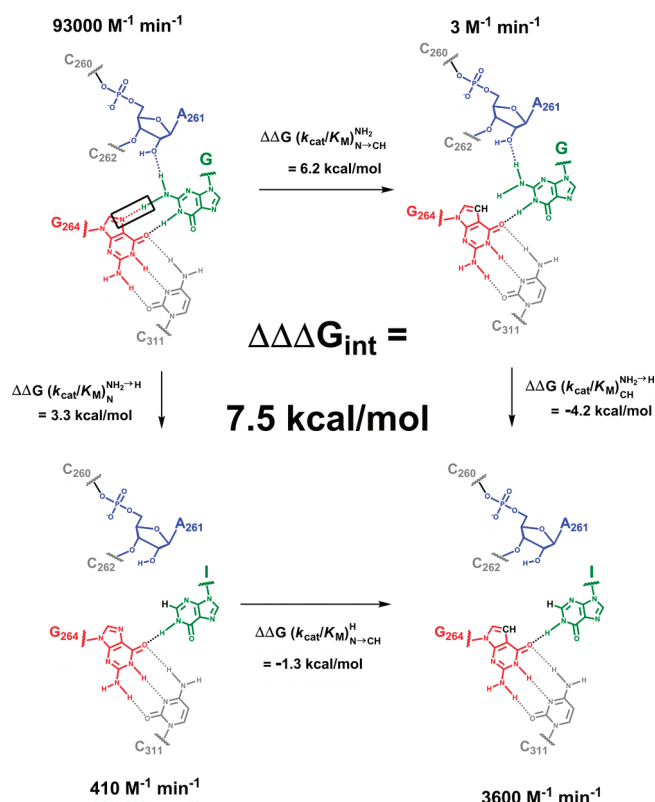


**Figure 3.** Testing the proposed contact between the exocyclic amino group of AUCG and the N7 atom of residue G264. The contact tested is highlighted by a black rectangle and corresponds to the red dashed line in Figure 2. Numbers with units of M<sup>-1</sup> min<sup>-1</sup> represent the second-order rate constant  $[(k_{\text{cat}}/K_M)^{\text{AUCG}}]$  for reactions of AUCG (top) or AUCI (bottom) with the WT (left) or G264deaza (right) ribozymes. Vertical arrows: differences in reactivity between AUCG and AUCI for the WT ribozyme (left) and G264deaza ribozyme (right). Horizontal arrows: differences in reactivity between the WT and G264deaza ribozymes when AUCG (top) or AUCI (bottom) is used as the nucleophile. Values of  $\Delta\Delta G$  are calculated from the relationship  $\Delta\Delta G = -RT \ln[\text{ratio}(k_{\text{cat}}/K_M)]$  and were rounded to a single decimal figure to take into account the experimental errors.  $\Delta\Delta\Delta G_{\text{int}}$  is the difference between  $\Delta\Delta G$  values on opposite sides of the cycle.

formed, as suggested by the structural data. Furthermore, the coupling energy ( $\Delta\Delta\Delta G_{\text{int}}$ ) of 7.5 kcal/mol is remarkably large. We therefore investigated the origin of this coupling.

#### A Physical Model for the Extremely Large Coupling Energy.

Site-directed mutagenesis that removes one hydrogen-bond partner in neutral hydrogen-bonded complexes typically gives energetic effects of 0.5–1.5 kcal/mol.<sup>42,43</sup> How then does the G264 N7 hydrogen bond to the exocyclic amino group of the G nucleophile give an energetic effect of 6.2 kcal/mol and a coupling energy of 7.5 kcal/mol (Figure 3)? Replacement of the nitrogen atom at the 7-position of residue G264 with a CH group introduces changes beyond the loss of the hydrogen-bond acceptor properties at the 7-position: The pK<sub>a</sub> of the purine N1 atom is altered,<sup>44</sup> stacking properties differ,<sup>45,46</sup> a larger volume is occupied by the CH group of 7-deazaguanosine compared to the N7 atom of G, and a hydrophobic group replaces a polar group. Because the nucleophilic G molecule does not interact directly with the N1 of G264 and does not stack with this residue, differences in the pK<sub>a</sub> and in the stacking properties of residue 264 would be predicted to affect reactivity of AUCG and AUCI to

the same extent and therefore would be unlikely to have large differential energetic effects and thus give little or no coupling energy. However, steric and polar differences could give differential effects and contribute to the observed coupling energy, as observed occasionally in other RNA systems.<sup>47</sup>

Simple consideration of van der Waals radii shows that replacement of the nitrogen atom at the 7-position of residue G264 with a CH group could introduce a steric or a polar clash between the hydrogen atom of the CH group and a hydrogen atom of the exocyclic amino group of the AUCG nucleophile (Supplemental Figure 1, Supporting Information). Such unfavorable interactions may result in weaker binding and, subsequent to binding, altered positioning of the AUCG nucleophile relative to the transferred phosphoryl group or the catalytic metal ions depicted in Figure 1b. This model predicts that AUCI, in which the exocyclic amino group is replaced by a smaller, apolar H atom, would relieve the unfavorable interaction and thus would react faster than AUCG in the G264deaza ribozyme. In agreement with this prediction, as noted above, AUCI reacts 1200-fold faster (corresponding to 4.2 kcal/mol) than AUCG with the G264deaza ribozyme (Figure 3, 3600 and 3 M<sup>-1</sup> min<sup>-1</sup>, respectively). An additional factor that could lead to increased reactivity of AUCI in the G264deaza ribozyme (relative to the WT ribozyme) would be easier desolvation of the 7-CH group of the G264deaza ribozyme than the N7 of the WT ribozyme.

Unfavorable steric or polar interactions might simply eliminate a single hydrogen bond. Alternatively, they might cause the loss of multiple interactions. For example, the interaction made by the other hydrogen atom of the exocyclic amino group of AUCG with the 2'-OH group of residue A261 of the WT ribozyme<sup>36</sup> might be broken to relieve a steric clash. To distinguish between these models, we measured the reactivity of a ribozyme containing both a CH group at the 7-position of G264 and a 2'-deoxy substitution at position A261 (i.e., the G264deaza/A261H ribozyme). If the interaction between the exocyclic amino group of AUCG and the 25'-OH group of residue A261 were not formed when the N7 atom of G264 is replaced by a CH group, then the G264deaza/A261H and the G264deaza ribozymes would react with the same second-order rate constant (Figure 4, red arrow). In contrast, if the interaction were still formed, the second-order rate constant of the G264deaza/A261H ribozyme would be expected to drop by 180-fold (3.3 kcal/mol), which corresponds to the energetic penalty observed for the A261 substitution alone (Figure 4, blue arrow).<sup>36</sup> In agreement with the former model, we found that the reaction of the G264deaza/A261H ribozyme is within 2-fold of that for the G264deaza ribozyme, corresponding to only 0.5 kcal/mol of destabilization from the second substitution rather than the 3.3 kcal/mol predicted for independent contributions (Figure 4). This result strongly suggests that the introduction of 7-deazaguanosine at position 264 leads to rearrangements that result in the weakening or loss of the interaction between the exocyclic amino group of AUCG and the 2'-OH group of residue A261 in the transition state.

The results presented above imply that the introduction of a CH group at the 7-position of residue 264 leads to structural rearrangements that alter the position of the AUCG nucleophile relative to other groups. The ribozyme appears to be unable to rearrange locally to accommodate the structural perturbation and maintain transition state stabilization, and the results therefore suggest a substantial rigidity in and around the G-binding site. To measure this energetic penalty along the reaction pathway, we monitored the coupling energy for the interaction between the

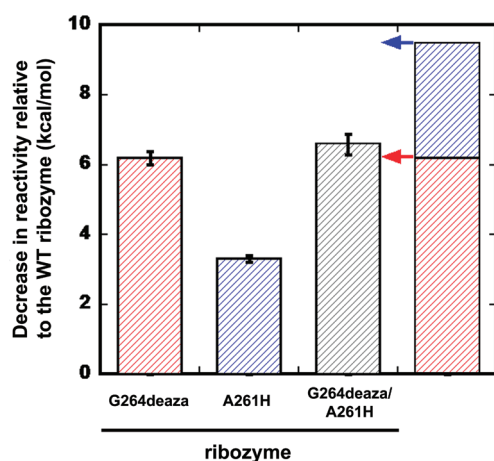


**Figure 4.** Decrease in reactivity of single and double modified ribozymes compared to the WT ribozyme. The three bars on the left represent the measured energetic penalty on the second-order rate constant from introducing a 7-deazaguanosine at position 264 (G264deaza, red), a 2'-H group at position 261 (A261H, blue), and the two groups simultaneously (G264deaza/A261H, gray), relative to the WT ribozyme. The stacked bar on the right represents the sum of the energetic penalties of the G264deaza and the A261H ribozymes. The arrows next to this bar represent the energetic penalty expected if the G264deaza and the A261H effects were fully coupled (red arrow) or fully independent (blue arrow). As described in the text, there is only a 0.5 kcal/mol difference between energetic penalty corresponding to the red arrow and the measured value for the G264deaza/A261H ribozyme.

exocyclic amino group of AUCG and the N7 atom of residue G264 in AUCG binding, S docking, and the chemical step, as described below.

**Tightening of the Network of Interactions along the Reaction Pathway.** We first determined the energetic penalty of removing the exocyclic amino group of G on binding of the nucleophile to the open complexes  $[(E \cdot S)_o]$  of the WT and G264deaza ribozymes. As noted above, binding to the open complex is expected to be identical to binding to the free enzyme<sup>13</sup> but is more convenient to measure. AUCG binding to the open complex of the G264deaza ribozyme is destabilized by 1.5 kcal/mol, relative to binding of the same nucleophile to the WT ribozyme (Figure 5a). This energetic penalty is about half of the energetic penalty arising from the use of AUCI as the nucleophile in reactions of the WT ribozyme (Figure 5a and ref 36). Because AUCI lacks two hydrogen bonds with the ribozyme, compared to AUCG, the result above suggests, most simply, that in the open complex of the G264deaza ribozyme AUCG forms only one hydrogen bond with the ribozyme (the one between the exocyclic amino group of the G nucleophile and an unknown group).<sup>26</sup> Consistent with this model, there is an additional penalty from removing the exocyclic amino group of AUCG for the G264deaza ribozyme (0.9 kcal/mol, Figure 5a). AUCI binds with the same affinities to the open complexes of the WT and the G264deaza ribozymes, as expected if no gross perturbations are introduced in the G264deaza ribozyme.

Quantitative analysis of all of the results for this reaction step, shown in Figure 5a, reveals a coupling energy of 1.5 kcal/mol (Figure 5a,  $\Delta\Delta\Delta G_{\text{int}}$ ), much smaller than the overall coupling energy of 7.5 kcal/mol (Figure 3). This result suggests that the  $(E \cdot S \cdot \text{AUCG})_o$  complex of the G264deaza ribozyme can readily accommodate via rearrangements and/or solvent reorganization

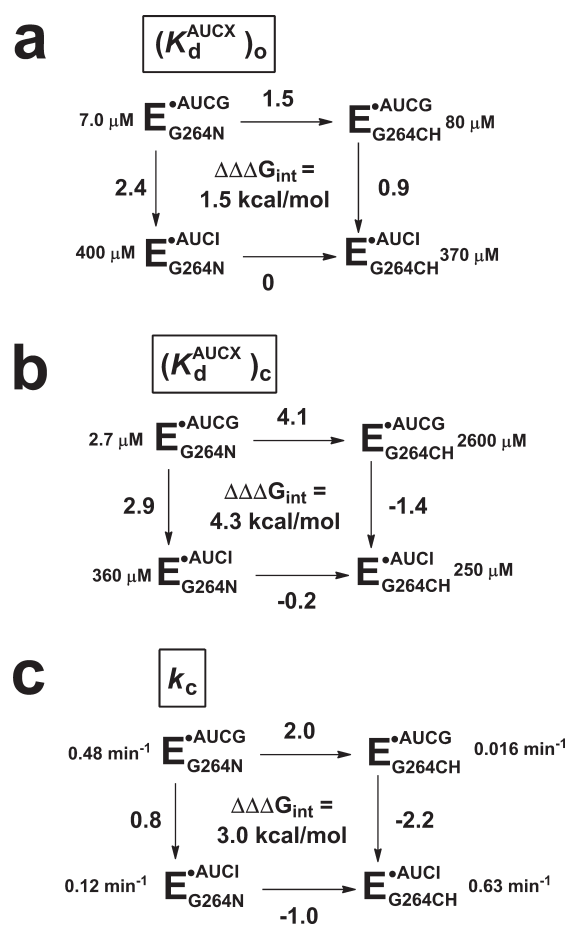


**Figure 5.** Testing individual reaction steps for the proposed contact between the exocyclic amino group of AUCG and the N7 atom of residue G264. Reactions for the WT ( $E_{\text{G264N}}$ ) or G264deaza ( $E_{\text{G264CH}}$ ) ribozymes with AUCG or AUCI. AUCX represents either AUCG or AUCI. The numbers next to each arrow represent the functional effect ( $\Delta\Delta G$  in kcal/mol) of either replacing the N7 of residue G264 with a CH group (horizontal arrows) or ablating the exocyclic amine of AUCG, by use of AUCI as the nucleophile (vertical arrows). Values of  $\Delta\Delta\Delta G_{\text{int}}$  are calculated by subtracting the value on the right from the value on the left or, equivalently, the value on the bottom from the value on the top. The individual reaction steps (defined in Figure 1a) are as follows: (a) nucleophile binding to the open complex  $[(K_d^{\text{AUCX}})_o]$ ; (b) nucleophile binding to the closed complex  $[(K_d^{\text{AUCX}})_c]$ ; and (c) the chemical step ( $k_c$ ).  $\Delta\Delta\Delta G$  values were rounded to a single decimal place to take in account the experimental errors. The sum of the coupling energies on the individual reaction steps matches the overall effect reported in Figure 3 (see Supporting Information).

the perturbation introduced by the CH group at the 7-position of residue 264, while maintaining other interactions formed between the G nucleophile and the ribozyme. Thus, the environment around the G nucleophile is relatively 'loose' or flexible in the open complex (Figure 6).

We next monitored the energetic penalty from removal of the exocyclic amino group of G on the binding affinity of the nucleophile for the closed complexes  $[(E \cdot S)_c]$  of the WT and G264deaza ribozymes. In this case, AUCG binding to the closed complex of the G264deaza ribozyme is destabilized by 4.1 kcal/mol, relative to binding of the same nucleophile to the WT ribozyme (Figure 5b), consistent with the loss of the additional contact between the nucleophile and the 2'-OH of A261 in the

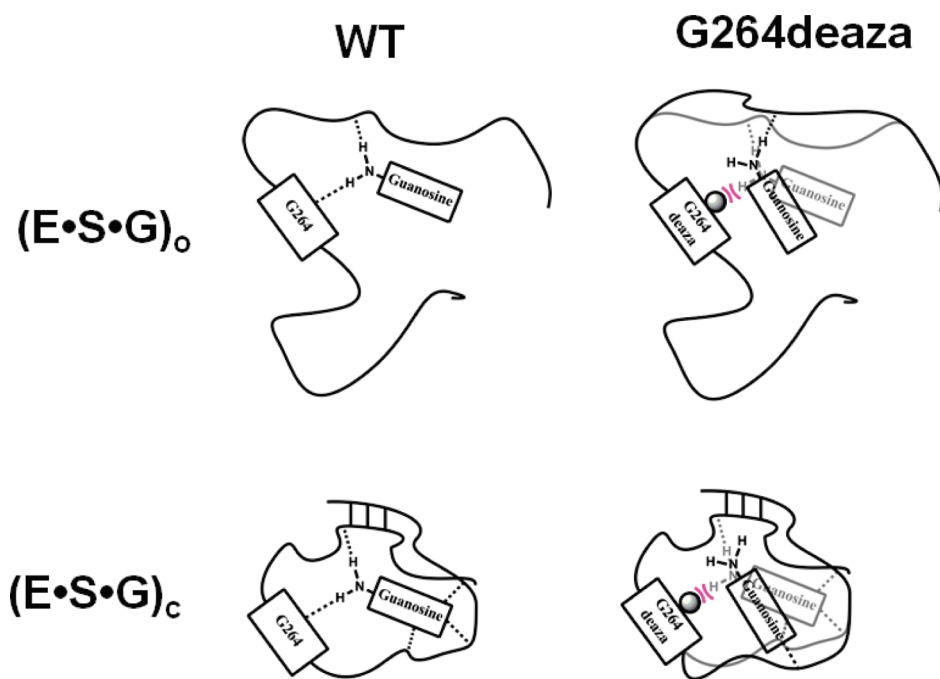


**Figure 6.** Schematic model of the differences between the G binding site of the WT ribozyme and that of the G264deaza ribozyme. Dashed lines represent interactions between the G and the ribozyme, and pink curved lines represent the unfavorable interaction between the 7-deaza group of the G264deaza ribozyme and the exocyclic amino group of the nucleophilic G. In the open complex there is sufficient flexibility to maintain the other interaction of the G exocyclic amine in the G264deaza ribozyme, but the tighter and more extensive network of interactions in the closed complex prevents reorientation of the other hydrogen-bond acceptor and thus leads to the loss of both hydrogen bonds in the G264deaza ribozyme.

G264deaza ribozyme (Figure 4). Surprisingly, this value is even larger than the 2.9 kcal/mol measured for the loss of the two hydrogen bonds made by the exocyclic amino group of AUCG (left vertical arrow in Figure 5b)<sup>15,26,36,48</sup> and suggests that more than two interactions are lost in the closed complex of the G264deaza ribozyme. We further investigate the reason for such large energetic effect below (see Introduction of 7-Deazaguanosine at Position 264 Perturbs the  $M_C$  Environment Section).

Unlike the open complex, the closed complex of the G264deaza ribozyme does not seem to be able to accommodate the unfavorable interaction arising from the N7 substitution at position 264. This inability suggests that in the closed complex the nucleophile binding energy derives from a tighter or more extensive network of interactions within the ribozyme's scaffold compared to the open complex (Figure 6). When the unfavorable interaction between the exocyclic amino group of AUCG and the CH group of the G264deaza ribozyme is removed, by using AUCI, the nucleophile binds tighter than AUCG, suggesting that the lack of the exocyclic amino group, which eliminates the unfavorable interaction, allows AUCI to maintain its position within the active site without disrupting the alignment of groups in the surrounding network of interactions.

The transition state for the reaction with AUCG is destabilized by 2.0 kcal/mol in the G264deaza ribozyme, relative to that in the WT ribozyme (Figure 5c). Thus, there is an additional penalty, not present in the closed complex, that arises as the closed complex proceeds to the transition state of the reaction. In the transition state for the chemical step, AUCI is again favored (by 2.2 kcal/mol) relative to AUCG in the G264deaza ribozyme, indicating that ablating the exocyclic amino group relieves an energetic penalty. These results reveal a large coupling energy between the exocyclic amine and G264 N7 in the transition state

(Figure 5c, 3.0 kcal/mol). Further, in this case AUCI reacts within the G264deaza ribozyme as fast as AUCG reacts within the WT ribozyme (0.63 and 0.48 min<sup>-1</sup>, Figure 5c). This result provides further support for the existence of a tight network of interactions: Once the unfavorable interactions are removed, other interactions surrounding the nucleophile appear to be sufficient to orient it for optimal catalysis. It is also possible that apolar interactions between the hydrophobic CH at position 264 and the hydrogen of AUCI might help alignment of the nucleophile in the chemical step.

The simplest explanation for the large effect on the chemical step is that the unfavorable interaction between AUCG and the CH group of 7-deazaguanosine at position 264 alters the positioning of the nucleophile and that the network of interactions surrounding the reactive elements makes it energetically costly to accommodate the modification without the loss of native interactions. The 2'- and 3'-oxygen atoms of the G nucleophile are involved in catalytic interactions (Figure 1b), so it is possible that an alteration in G positioning would affect interactions with these atoms. To test this possibility, we determined whether the contact between the 2'-oxygen and the catalytic metal ion  $M_C$  is altered in the G264deaza ribozyme.

**Introduction of 7-Deazaguanosine at Position 264 Perturbs the  $M_C$  Environment.** Previous results with the WT and several modified ribozymes have shown that 2'-aminoguanosine reacts slower than G and that metal ions, such as  $Mn^{2+}$  and  $Cd^{2+}$ , stimulate the reactivity of 2'-aminoguanosine, relative to that of G.<sup>34,35,49,50</sup> Because  $Mn^{2+}$  and  $Cd^{2+}$  interact better than  $Mg^{2+}$  with nitrogen atoms, these and other observations suggested that a metal ion interacts with the 2'-group of the G nucleophile. Increasing  $Mn^{2+}$  concentration results in increased  $Mn^{2+}$ -occupancy of site C (Figure 1b), which allows a more



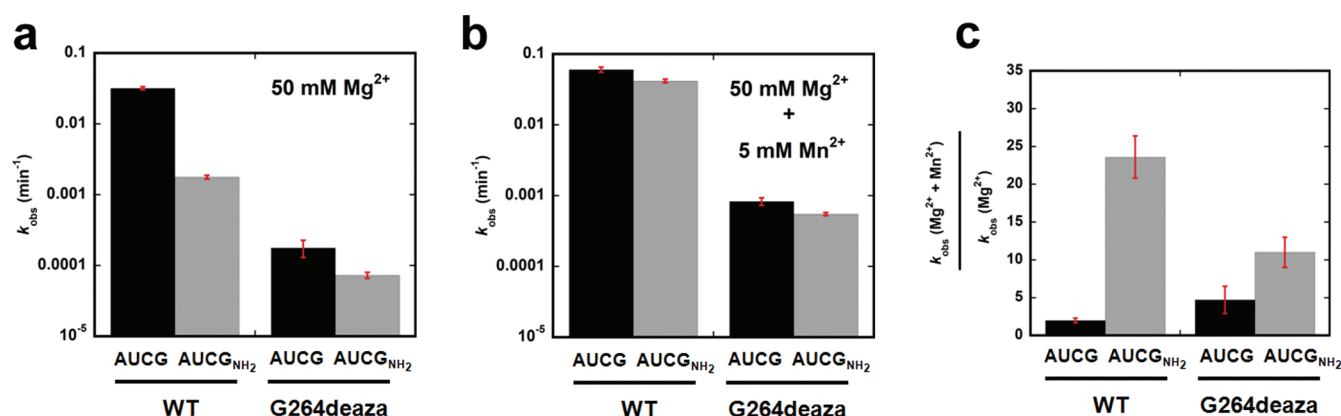


**Figure 7.** Observed rate constant for reactions of AUCG and AUCG<sub>2'-NH<sub>2</sub></sub> with the WT and G264deaza ribozymes. Reactions were carried out with 0.6  $\mu\text{M}$  nucleophile for the WT ribozyme and with 6  $\mu\text{M}$  nucleophile for the G264deaza ribozyme, starting from the (E·S)<sub>0</sub> complex in both cases. Reactions of AUCG are represented by the black bars, and reactions of AUCG<sub>2'-NH<sub>2</sub></sub> are represented by gray bars. (a) Rate constants for reactions in 50 mM Mg<sup>2+</sup>. (b) Rate constants for reactions in 50 mM Mg<sup>2+</sup> and 5 mM Mn<sup>2+</sup>. (c) Ratio between rate constants in panels (b) and (a). Rate constants for reactions at intermediate Mn<sup>2+</sup> concentrations are given in Supplemental Figure S4, Supporting Information.

favorable interaction with the amino group of 2'-aminoguanosine in the transition state compared to Mg<sup>2+</sup>.

We have used the above information to test whether the contact between the 2'-oxygen and M<sub>C</sub> is suboptimal for function in the G264deaza ribozyme. Specifically, we determined the effect of addition of Mn<sup>2+</sup> ions on the reactions of AUCG and AUCG<sub>2'-NH<sub>2</sub></sub>, a G analog containing a 2'-amino group instead of a 2'-hydroxyl, with the WT and G264deaza ribozymes. If the interaction between M<sub>C</sub> and the 2'-moiety of the nucleophile were perturbed in the G264deaza ribozyme, then a lessened deleterious effect upon introduction of the 2'-amino group on the nucleophile in the G264deaza ribozyme compared to the WT ribozyme would be predicted. Further, if there were altered positioning of M<sub>C</sub> and of the 2'-moiety of the nucleophilic G in the G264deaza ribozyme, then Mn<sup>2+</sup> might not be able to rescue the reactivity of AUCG<sub>2'-NH<sub>2</sub></sub>. As described below, both predictions were met.

When only Mg<sup>2+</sup> is present, AUCG<sub>2'-NH<sub>2</sub></sub> reacts with the WT (E·S)<sub>0</sub> complex ~20-fold slower than AUCG. In contrast, AUCG<sub>2'-NH<sub>2</sub></sub> reacts with the G264deaza (E·S)<sub>0</sub> complex within 3-fold of the AUCG rate (Figure 7a). Further, addition of 5 mM Mn<sup>2+</sup> stimulates the reactivity of AUCG<sub>2'-NH<sub>2</sub></sub> with the (ES)<sub>0</sub> complex of the WT ribozyme, relative to that of AUCG, such that now the reaction rates are within 2-fold (Figure 7b). This corresponds to a 12-fold greater stimulation of AUCG<sub>2'-NH<sub>2</sub></sub> than AUCG; in contrast, this stimulation is only 2-fold in the G264deaza ribozyme (Figure 7c). The ~5-fold Mn<sup>2+</sup> stimulation for reactions of both AUCG and AUCG<sub>2'-NH<sub>2</sub></sub> with the G264deaza ribozyme (Figure 7c and Supplemental Figure 4, Supporting Information) is consistent with the effect from a distinct metal ion, referred to as M<sub>D</sub>, which stabilizes the closed complex.<sup>51</sup> The simplest model to explain these results is that the interaction between M<sub>C</sub> and the 2'-moiety of the nucleophile is absent or substantially altered in the G264deaza ribozyme. Such a perturbed interaction may be responsible for the 30-fold slower chemical step for the reaction of the G264deaza ribozyme with AUCG relative to the WT ribozyme (Figure 5c).

## DISCUSSION

Since the original discovery by Buchner that fermentation can occur without intact cells,<sup>52</sup> many enzymes have been identified.

For many classes of enzymes, researchers have established reasonable reaction mechanisms based on the chemical properties of individual active site functional groups in isolation.<sup>53,54</sup> However, active site residues are not present in enzymes as disjointed entities, and structural inspections of enzymes almost inevitably reveal intricate networks of interactions surrounding active sites. These networks of interactions surrounding the active sites can be important for function. For example, trypsin was converted to chymotrypsin by changing surface loops that do not interact with the substrate;<sup>55</sup> statistical and mutational analysis of the PDZ domain family uncovered networks of interactions that allow energetic coupling between distal residues;<sup>56</sup> 16 of the 17 mutations needed to switch the specificity of an aminotransferase from aspartate to valine involve residues located outside the active site;<sup>57</sup> and the activity of a catalytic antibody was increased 100-fold without any change in the residues directly contacting the substrate.<sup>58</sup> Guided by structural data, chemical approaches, such as specific replacements of atoms involved in these putative networks, in conjunction with careful thermodynamic and kinetic analysis of the resulting functional effects, can be used to understand the origin of energetic coupling at an atomic level.

RNA enzymes are excellent systems for these types of studies because of their amenability to single-atom substitution<sup>59</sup> and the highly developed kinetic and thermodynamic frameworks available to facilitate interpretation. For the group I intron in particular, functional and structural studies have uncovered the groups directly involved in catalysis and the architecture of the substrates' binding sites.<sup>4</sup> In this ribozyme, previous functional<sup>16</sup> and structural<sup>19–21,24</sup> data predicted an interaction between the N7 of residue G264 and the exocyclic amino group of the nucleophilic G. Our results, based on the double mutant cycle shown in Figure 3, not surprisingly, provide experimental evidence for this interaction. However, the additional functional and structural consequences arising from the introduction of a CH group at the 7-position of residue 264 have revealed remarkable unforeseen properties of an RNA active site, strikingly large energetic effects and loss of interactions in addition to the one monitored.

We have shown that the introduction of a CH group at the 7-position of residue 264 affects binding of AUCG to the open complex of the ribozyme by 1.5 kcal/mol, an energetic effect



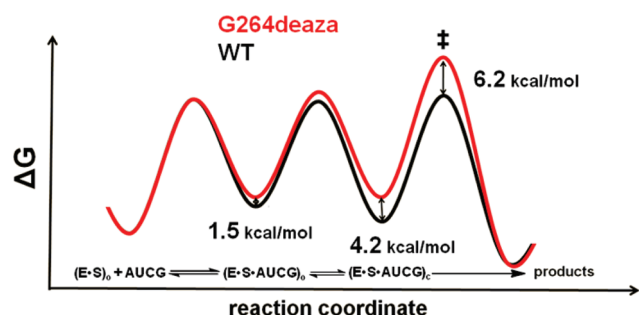


**Figure 8.** Free energy profiles for the WT ribozyme (black line) and the G264deaza ribozyme (red line) obtained from the data in Figure 5. Free energy differences were obtained from the rate and equilibrium constants using the standard conversions:  $\Delta G^\ddagger = -RT \ln(k(h)/(k_B T))$  and  $\Delta G = -RT \ln K_{eq}$ . The profiles are qualitative, but the noted values of  $\Delta\Delta G$  are quantitative.

often seen for the loss of a single hydrogen bond.<sup>42,43</sup> This energetic effect is depicted in the free energy profile of Figure 8 by the difference in energy between the  $(E \cdot S \cdot AUCG)_0$  complexes of the WT (black line) and the G264deaza (red line) ribozymes. This result suggests that, despite the differences in size and polarity between the native nitrogen atom and the introduced CH group, the remaining interactions between the nucleophilic G and the ribozyme are the same in the WT and G264deaza ribozymes. These interactions likely include the hydrogen bond between the N1 of G and the O6 of G264<sup>16</sup> (shown in magenta in Figure 9, top) and a hydrogen bond between the exocyclic amino group of G and an unknown partner (not shown in Figure 9).<sup>60</sup> Thus, the G nucleophile communicates within a relatively small, loose network of residues, highlighted in magenta in the top panel of Figure 9.

When the oligonucleotide substrate docks in the ribozyme's active site, forming tertiary interactions with the ribozyme's backbone and contacting the catalytic metal ions,<sup>4,22</sup> the nucleophilic G forms additional interactions with the 2'-OH group of residue A261 (via its exocyclic amino group)<sup>26</sup> and with the catalytic metal ion  $M_C$ .<sup>22,49</sup> This establishes additional connectivity between the G nucleophile and parts of the active site, highlighted in magenta in the middle panel of Figure 9. Thus, the G nucleophile communicates with a larger network of interactions in the closed complex than in the open complex (cf., Figure 9, top and middle panels), which includes the bonds shown in magenta in middle panel of Figure 9. An oxygen atom of the phosphoryl group connecting residues A261 and C262 is a ligand of  $M_C$ <sup>21,22,24,34</sup> and is thus part of this network, and the bases of A261 and C262 stack above and below the guanine base of the bound G.<sup>20–22,24</sup> Further, the base of A306 stacks over A261,<sup>20,21</sup> and its phosphoryl oxygen atoms ligand both  $M_C$  and  $M_A$ .<sup>22,24,35</sup> Such a network might be important for selective recognition of G for catalysis and may help precisely position the reactive groups for the chemical step.

The energetic penalty of 4.2 kcal/mol on AUCG binding to the closed complex of the ribozyme, arising from the introduction of a CH group at the 7-position of residue 264, is larger than the value typically observed from the loss of a single hydrogen bond (0.5–1.5 kcal/mol).<sup>42,43</sup> This energetic penalty is significantly larger than the penalty measured in the open complex, as shown in Figure 8. The results shown above (see Figures 4 and 7) strongly suggest that the hydrogen bond with residue A261 and the contact with  $M_C$  are perturbed in the G264deaza ribozyme.

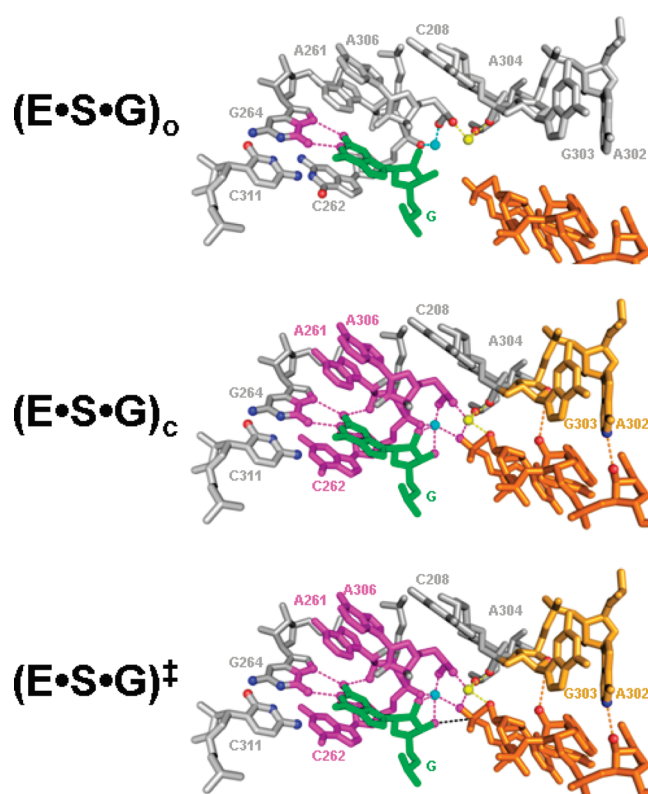


**Figure 9.** The network of interactions around the nucleophilic G tightens and becomes more extensive in the transition state of the reaction. The nucleophilic G is shown in green; residues of the oligonucleotide substrate are in orange; ribozyme residues interacting with the C-2 and U-3 residues of the oligonucleotide substrate in the docked conformation are in dark yellow; and other residues are in gray.  $M_A$  is in yellow, and  $M_C$  is in cyan. The bond formed in the transition state is indicated by a black dashed line. Residues for which there is evidence for energetic or functional communication with the G nucleophile in the WT ribozyme are shown in magenta; interactions involved in the communication networks are shown by magenta dashed lines; and specific atoms involved in this network are also in magenta. Other atoms known to be important for function are shown in red (oxygen) or in blue (nitrogen). This figure was generated using Pymol (Schrödinger, LLC) and the 3BO3 *Azoarcus* structural model. Residues are numbered using the corresponding numbers from the *Tetrahymena* group I ribozyme.

The inability of the G nucleophile to rearrange to accommodate the atomic change in the G264deaza ribozyme without disruption of distal interactions strongly implies the presence of a tight, rigid network of interactions around the G nucleophile (Figure 9, residues in magenta in the middle panel).

If the precise positioning of the nucleophilic G were not important for the reaction, then the chemical step for the G264deaza ribozyme would be unaffected by the deaza substitution. In contrast, the  $\sim 30$ -fold slower reactivity in the chemical step and the lack of rescue of  $AUCG_{2'-NH_2}$  by  $Mn^{2+}$  strongly suggests that the nucleophilic G does not rearrange within the active site to form the most favorable contact with  $M_C$  and likely sits in a suboptimal position for attack on the transferred phosphoryl group. This is an additional penalty of  $\sim 2.0$  kcal/mol, which is not present in the closed complex and brings the total destabilization given by the deaza substitution at position G264 to 6.2 kcal/mol (Figure 8). Our results suggest that such large energetic penalty is given by the difficulty to rearrange the tight

network of interactions that impart catalysis once even a remote aspect of that network is perturbed (shown in magenta in the bottom panel of Figure 9).

In contrast to the evidence for tight coupling from the substitutions studied herein, substitutions of sulfur atoms for active site oxygen ligands of metal ions and of  $\text{Cd}^{2+}$  for  $\text{Mg}^{2+}$ , which both introduce groups larger than the native ones, have smaller effects on reactivity.<sup>35</sup> Perhaps the multiple rotatable bonds around the phosphoryl groups ease relaxation at these sites, whereas the multiple reinforcing hydrogen bonding, stacking, and covalent linkages associated with G binding leave less room for rearrangement. In addition, hydrogen-bonding interactions require precise directionality, whereas interactions with metal ions may be more permissive.

Like protein enzymes, ribozymes use binding interactions to position reactive groups, substrates, and catalytic residues.<sup>3,5,6,15</sup> We have used chemical modifications and functional tests to show that in the *Tetrahymena* ribozyme at least some of these binding interactions are used to establish a tight network of interactions around the active site. Ultimately, these networks may be used by ribozymes as well as protein enzymes to limit dynamics and provide the precise positioning of the substrates and the catalytic residues that appear to contribute substantially to the remarkable catalytic power of enzymes.<sup>61</sup> Such networks, by connecting distal regions of an RNA to active centers, also introduce the potential for highly responsive, long-range conformational coupling, as occurs in RNA-based machinery, such as the ribosome and the spliceosome.

## ■ ASSOCIATED CONTENT

**S Supporting Information.** Figures with the representation of possible clashes in the G264deaza ribozyme, analysis of the coupling energy on the individual reaction steps, plots of  $k_{\text{obs}}$  as a function of [AUCG] in the closed complexes of the WT and G264deaza ribozyme, and plots of  $k_{\text{obs}}$  as a function of  $[\text{Mn}^{2+}]$  for reactions of the open complexes of the WT and G264deaza ribozymes with AUCG and AUCG<sub>NH<sub>2</sub></sub>. This material is available free of charge via the Internet at <http://pubs.acs.org>.

## ■ AUTHOR INFORMATION

### Corresponding Author

[herschla@stanford.edu](mailto:herschla@stanford.edu)

### Present Addresses

<sup>||</sup>Department of Chemistry and Biochemistry, College of Charleston, Charleston, South Carolina, United States.

## ■ ACKNOWLEDGMENT

This work was supported by a grant from the NIH (GM 49243) to D.H. We thank members of the Herschlag lab for helpful comments on the manuscript.

## ■ REFERENCES

- (1) Hoogstraten, C. G.; Sumita, M. *Biopolymers* **2007**, *87*, 317.
- (2) Lilley, D. M. *Trends Biochem. Sci.* **2003**, *28*, 495.
- (3) Narlikar, G. J.; Herschlag, D. *Annu. Rev. Biochem.* **1997**, *66*, 19.
- (4) Hougland, J. L.; Piccirilli, J. A.; Forconi, M.; Lee, J.; Herschlag, D. In *The RNA World*; 3rd ed.; Gesteland, R. F., Cech, T. R., Atkins, J. F., Eds.; Cold Spring Harbor Laboratory Press: Cold Spring Harbor, NY, 2006.

- (5) Narlikar, G. J.; Gopalakrishnan, V.; McConnell, T. S.; Usman, N.; Herschlag, D. *Proc. Natl. Acad. Sci. U.S.A.* **1995**, *92*, 3668.
- (6) Hertel, K. J.; Peracchi, A.; Uhlenbeck, O. C.; Herschlag, D. *Proc. Natl. Acad. Sci. U.S.A.* **1997**, *94*, 8497.
- (7) Sigler, P. B. *Annu. Rev. Biophys. Bioeng.* **1975**, *4*, 477.
- (8) Antonioli, A. H.; Cochran, J. C.; Lipchick, S. V.; Strobel, S. A. *RNA* **2010**, *16*, 762.
- (9) Santalucia, J.; Kierzek, R.; Turner, D. H. *Science* **1992**, *256*, 217.
- (10) Herschlag, D.; Cech, T. R. *Biochemistry* **1990**, *29*, 10159.
- (11) Bevilacqua, P. C.; Turner, D. H. *Biochemistry* **1991**, *30*, 10632.
- (12) Herschlag, D. *Biochemistry* **1992**, *31*, 1386.
- (13) McConnell, T. S.; Cech, T. R.; Herschlag, D. *Proc. Natl. Acad. Sci. U.S.A.* **1993**, *90*, 8362.
- (14) Latham, J. A.; Cech, T. R. *Science* **1989**, *245*, 276.
- (15) Bass, B. L.; Cech, T. R. *Nature* **1984**, *308*, 820.
- (16) Michel, F.; Hanna, M.; Green, R.; Bartel, D. P.; Szostak, J. W. *Nature* **1989**, *342*, 391.
- (17) Ortoleva-Donnelly, L.; Szewczak, A. A.; Gutell, R. R.; Strobel, S. A. *RNA* **1998**, *4*, 498.
- (18) Yarus, M.; Illangsekare, M.; Christian, E. J. *Mol. Biol.* **1991**, *222*, 995.
- (19) Adams, P. L.; Stahley, M. R.; Kosek, A. B.; Wang, J.; Strobel, S. A. *Nature* **2004**, *430*, 45.
- (20) Golden, B. L.; Kim, H.; Chase, E. *Nature Struct. Mol. Biol.* **2005**, *12*, 82.
- (21) Guo, F.; Gooding, A. R.; Cech, T. R. *Mol. Cell* **2005**, *16*, 351.
- (22) Lipchick, S. V.; Strobel, S. A. *Proc. Natl. Acad. Sci. U.S.A.* **2008**, *105*, 5699.
- (23) Paukstelis, P. J.; Chen, J. H.; Chase, E.; Lambowitz, A. M.; Golden, B. L. *Nature* **2008**, *451*, 94.
- (24) Stahley, M. R.; Strobel, S. A. *Science* **2005**, *309*, 1587.
- (25) Dai, Q.; Deb, S. K.; Hougland, J. L.; Piccirilli, J. A. *Bioorg. Med. Chem.* **2006**, *14*, 705.
- (26) Forconi, M.; Sengupta, R. N.; Piccirilli, J. A.; Herschlag, D. *Biochemistry* **2010**, *49*, 2753.
- (27) Moore, M. J.; Sharp, P. A. *Science* **1992**, *256*, 992.
- (28) Mei, R.; Herschlag, D. *Biochemistry* **1996**, *35*, 5796.
- (29) Pyle, A. M.; Mcswiggen, J. A.; Cech, T. R. *Proc. Natl. Acad. Sci. U.S.A.* **1990**, *87*, 8187.
- (30) Knitt, D. S.; Herschlag, D. *Biochemistry* **1996**, *35*, 1560.
- (31) Horovitz, A. *Folding Des.* **1996**, *1*, R121.
- (32) Strobel, S. A.; Ortoleva-Donnelly, L. *Chem. Biol.* **1999**, *6*, 153.
- (33) Szewczak, A. A.; Kosek, A. B.; Piccirilli, J. A.; Strobel, S. A. *Biochemistry* **2002**, *41*, 2516.
- (34) Hougland, J. L.; Kravchuk, A. V.; Herschlag, D.; Piccirilli, J. A. *PLoS Biol.* **2005**, *3*, 1536.
- (35) Forconi, M.; Lee, J.; Lee, J. K.; Piccirilli, J. A.; Herschlag, D. *Biochemistry* **2008**, *47*, 6883.
- (36) Forconi, M.; Sengupta, R. N.; Liu, M. C.; Sartorelli, A. C.; Piccirilli, J. A.; Herschlag, D. *Angew. Chem., Int. Ed.* **2009**, *48*, 7171.
- (37) Pitha, P. M.; Huang, W. M.; Ts'o, P. O. *Proc. Natl. Acad. Sci. U.S.A.* **1968**, *61*, 332.
- (38) Moran, S.; Kierzek, R.; Turner, D. H. *Biochemistry* **1993**, *32*, 5247.
- (39) Russell, R.; Herschlag, D. *RNA* **1999**, *5*, 158.
- (40) Narlikar, G. J.; Bartley, L. E.; Koshla, M.; Herschlag, D. *Biochemistry* **1999**, *38*, 14192.
- (41) Shi, X.; Mollova, E. T.; Pljevaljcic, G.; Millar, D. P.; Herschlag, D. *J. Am. Chem. Soc.* **2009**, *131*, 9571.
- (42) Fersht, A. R.; Shi, J. P.; Knill-Jones, J.; Lowe, D. M.; Wilkinson, A. J.; Blow, D. M.; Brick, P.; Carter, P.; Waye, M. M.; Winter, G. *Nature* **1985**, *314*, 235.
- (43) Turner, D. H.; Sugimoto, N.; Kierzek, R.; Dreiker, S. D. *J. Am. Chem. Soc.* **1987**, *109*, 3783.
- (44) Seela, F.; Chen, Y. M. *Nucleic Acids Res.* **1995**, *23*, 2499.
- (45) Seela, F.; Tranthi, Q. H.; Franzen, D. *Biochemistry* **1982**, *21*, 4338.
- (46) Sistare, M. F.; Codden, S. J.; Heimlich, G.; Thorp, H. H. *J. Am. Chem. Soc.* **2000**, *122*, 4742.

- (47) Siegfried, N. A.; Kierzek, R.; Bevilacqua, P. C. *J. Am. Chem. Soc.* **2010**, *132*, 5342.
- (48) McConnell, T. S.; Cech, T. R. *Biochemistry* **1995**, *34*, 4056.
- (49) Shan, S.; Herschlag, D. *Biochemistry* **1999**, *38*, 10958.
- (50) Sjogren, A. J.; Petterson, E.; Sjoberg, B. M.; Stromberg, R. *Nucleic Acids Res.* **1997**, *25*, 648.
- (51) Shan, S.; Herschlag, D. *RNA* **2000**, *6*, 795.
- (52) Buchner, E. F. *Ber. Dt. Chem. Ges.* **1897**, *30*, 117.
- (53) McMurry, J.; Begley, T. *The Organic Chemistry of Biological Pathways*; Roberts & Company: Greenwood Village, CO, 2005.
- (54) Fersht, A. *Structure and Mechanism in Protein Science*; W.H. Freeman and Company: New York, 1999.
- (55) Hedstrom, L.; Szilagyi, L.; Rutter, W. J. *Science* **1992**, *255*, 1249.
- (56) Lockless, S. W.; Ranganathan, R. *Science* **1999**, *286*, 295.
- (57) Oue, S.; Okamoto, A.; Yano, T.; Kagamiyama, H. *J. Biol. Chem.* **1999**, *274*, 2344.
- (58) Patten, P. A.; Gray, N. S.; Yang, P. L.; Marks, C. B.; Wedemayer, G. J.; Boniface, J. J.; Stevens, R. C.; Schultz, P. G. *Science* **1996**, *271*, 1086.
- (59) Das, S. R.; Fong, R.; Piccirilli, J. A. *Curr. Opin. Chem. Biol.* **2005**, *9*, 585.
- (60) The second hydrogen bond with the 2'-OH of residue A261 that is formed in the closed complex is not formed in the open complex, but the 2.4 kcal/mol loss of binding energy associated with the removal of the exocyclic amino group of G suggests the loss of two hydrogen bonds, as described in ref 26.
- (61) Wolfenden, R. *Mol. Cell. Biochem.* **1974**, *3*, 207.